GLIA

GLIA 59:499–510 (2011)

Human Glial-Restricted Progenitors Survive, Proliferate, and Preserve Electrophysiological Function in Rats with Focal Inflammatory Spinal Cord Demyelination

PIOTR WALCZAK,[1,2]* ANGELO H. ALL,[3,4] NIDHI RUMPAL,[1,2] MICHAEL GORELIK,[1,2] HEECHUL KIM,[1,2] ANIL MAYBHATE,[4] GRACEE AGRAWAL,[4] JAMES T. CAMPANELLI,[5] ASSAF A. GILAD,[1,2] DOUGLAS A. KERR,[2,3] AND JEFF W. M. BULTE[1,2,4,6]

[1]*Russell H. Morgan Department of Radiology and Radiological Science, Division of MR Research, The Johns Hopkins University School of Medicine, Baltimore, Maryland*

[2]*Cellular Imaging Section and Vascular Biology Program, Institute for Cell Engineering, The Johns Hopkins University School of Medicine, Baltimore, Maryland*

[3]*Department of Neurology, The Johns Hopkins University School of Medicine, Baltimore, Maryland*

[4]*Department of Biomedical Engineering, The Johns Hopkins University School of Medicine, Baltimore, Maryland*

[5]*Q Therapeutics, Inc., Salt Lake City, Utah*

[6]*Department of Chemical and Biomolecular Engineering, The Johns Hopkins University School of Medicine, Baltimore, Maryland*

KEY WORDS
myelination; glial precursors; transplantation; spinal cord; electrophysiology

ABSTRACT
Transplantation of glial progenitor cells results in transplant-derived myelination and improved function in rodents with genetic dysmyelination or chemical demyelination. However, glial cell transplantation in adult CNS inflammatory demyelinating models has not been well studied. Here we transplanted human glial-restricted progenitor (hGRP) cells into the spinal cord of adult rats with inflammatory demyelination, and monitored cell fate in chemically immunosuppressed animals. We found that hGRPs migrate extensively, expand within inflammatory spinal cord lesions, do not form tumors, and adopt a mature glial phenotype, albeit at a low rate. Human GRP-transplanted rats, but not controls, exhibited preserved electrophysiological conduction across the spinal cord, though no differences in behavioral improvement were noted between the two groups. Although these hGRPs myelinated extensively after implantation into neonatal shiverer mouse brain, only marginal remyelination was observed in the inflammatory spinal cord demyelination model. The low rate of transplant-derived myelination in adult rat spinal cord may reflect host age, species, transplant environment/location, and/or immune suppression regime differences. We conclude that hGRPs have the capacity to myelinate dysmyelinated neonatal rodent brain and preserve conduction in the inflammatory demyelinated adult rodent spinal cord. The latter benefit is likely dependent on trophic support and suggests further exploration of potential of glial progenitors in animal models of chronic inflammatory demyelination.

INTRODUCTION

Demyelinating disorders of the central nervous system (CNS), such as transverse myelitis (TM) or multiple sclerosis (MS), remain a major cause of neurological disability among young adults. The pathogenesis of both TM and MS is characterized by inflammation, and oligodendrocyte and myelin destruction with initial sparing of axons. Extended periods of demyelination or repetitive inflammatory insults, such as those observed in MS, lead to axonal damage and result in irreversible loss of neurological function (Kerr and Ayetey, 2002; Lucchinetti et al., 1998). Therapeutic approaches for demyelinating disorders are primarily directed toward attenuating inflammatory/immune-mediated destruction of myelin by immunosuppressive or immunomodulatory agents (Jacobs et al., 1996; Kazatchkine and Kaveri, 2001). Such treatments prove only partially effective and, although it is possible to modify disease course and reduce the extent or slow the progression of disability, it is not possible, as yet, to prevent the progression of disability or to reverse prior disability. Evidence is mounting that patients who suffer from demyelinating conditions can benefit from cell replacement therapy (Goldman, 2005).

Recently, numerous preclinical studies have been performed using glial-restricted progenitor cells (GRPs). GRPs are derived from mid-gestation CNS tissue [Day 13.5 in rats (Rao et al., 1998) and 19–22 gestational weeks in humans]. The ability of these cells to form astrocytes and oligodendrocytes opens the possibility of their therapeutic use for several diseases, including white matter diseases (Windrem et al., 2008) and neurodegenerative diseases such as ALS (Maragakis et al., 2005). Several studies have demonstrated robust myelination by hGRP transplants into the neonatal dysmyeli-

Grant sponsor: NIH; Grant number: RO1 NS045062; Grant sponsor: NMSS; Grant number: RG3630; Grant sponsor: TEDCO; Grant numbers: MSCRFE0155, MSCRFII0193, MSCRFII0159, MSCRFII0190; Grant sponsor: Q Therapeutics, Inc.

*Correspondence to: Piotr Walczak, M.D., Assistant Professor, The Russell H. Morgan Department of Radiology and Radiological Science, Division of MR Research, Institute for Cell Engineering, The Johns Hopkins University School of Medicine, Broadway Research Building Rm 649, 733 N Broadway, Baltimore, MD 21205, USA. E-mail: pwalczak@mri.jhu.edu

Received 23 March 2010; Accepted 9 November 2010

DOI 10.1002/glia.21119

Published online 29 December 2010 in Wiley Online Library (wileyonlinelibrary.com).

nated shiverer mouse brain. The literature on the transplantation of GRPs into adult hosts is limited to rodent cell sources (Gregori et al., 2002; Han et al., 2004; Maragakis et al., 2005): to date, testing of hGRPs in an adult host has not been reported.

Here, we performed a study of grafting, in parallel, hGRPs into the demyelinated adult rat spinal cord and the neonatal myelin deficient *shi/shi* immune deficient *rag2*$^{-/-}$ mouse brain. This allows us to evaluate and compare the capabilities of our source hGRPs in two environments that differ in their innate ability for new myelination. In both developing mouse brain and adult rat spinal cord, hGRPs survive, expand, and migrate extensively. In both environments, hGRPs transition through the stage of Olig2+ oligodendrocyte precursor cell (OPC) development. In mice, the initial myelination by human cells is observed at 6 weeks after transplantation and is quite robust by Week 13. In rats, remyelination of the lesion is not achieved; however, few of the transplanted hGRPs become MBP-expressing oligodendrocytes 14 weeks after grafting. Moreover, electrophysiological measurements of somatosensory evoked potentials in lesioned rats reveal improvement in axonal conductivity toward the end of the experiment, indicating a positive effect of the cell therapy.

To our knowledge this is the first study evaluating the therapeutic potential of hGRPs in an adult rat model of focal inflammatory demyelination (such as occurs in transverse myelitis), while performing a detailed comparison of engraftment and cell differentiation to that occurring in the developing dysmyelinated brain.

MATERIALS AND METHODS

Animals

Adult female Lewis rats (Harlan), with an average body weight of 200–220 g, and neonatal (P1) *rag2*$^{-/-}$ shiverer *shi/shi* mice (1.4–1.9 g; inhouse colony) were used in these experiments. Animals were housed under an artificial light-dark cycle (12-h light and 12-h dark) and had access to food and water ad libitum. All experimental procedures were in accordance with the guidance provided in the Rodent Survival Surgery manual and were approved by our Institutional Animal Care and Use Committee.

Human Glial Resticted Progenitor (GRP) Preparation

Human GRPs were isolated from fetal cadaver brain tissue (gestational age 18–24 weeks) as previously described (Sandrock et al., 2010). Briefly, tissue was enzymatically and manually dissociated to yield a single cell suspension containing the GRPs. This single cell suspension was subject to immunomagnetic purification (Miltenyi Biotec) using the mouse monoclonal antibody A2B5 (an IgM antibody that recognizes c-series gangliosides on the cell surface of hGRPs; (Saito et al., 2001), and microbead-conjugated anti-mouse IgM secondary antibody. In addition to published isolation methods (Sandrock et al., 2010), positively selected cells were cultured for 20 days (three passages) in DMEM/F12/with N1 supplement and bFGF, harvested with TrypLE (Invitrogen), cryopreserved in ProFreeze/15% DMSO, and stored in vapor phase liquid nitrogen. This hGRP cell preparation has also been referred to as Q-Cells®.

Cell Transplantation: Neonatal Mice

Postnatal day 1 *rag2*$^{-/-}$ *shi/shi* mice were cryoanesthetized by brief submersion in ice. They were then stabilized in a stereotactic frame. Cells suspended in Hanks' Balanced Salt Solution at a concentration of 1×10^5 cells μL^{-1} were loaded into a Hamilton syringe with attached 31-G needle. The needle was lowered into the presumptive lateral ventricle of the brain and 4 μL of cell suspension was infused over the course of 1 min.

Cell Transplantation: Focal Myelitis Rat Model

Six to eight days after lesion induction (see below), hGRPs were transplanted into the spinal cord dorsal white matter 0.7 mm below the ventral surface at level T9. A total of 4×10^5 cells were injected with two bi-lateral injections of 2×10^5 cells/2 μL. The control group received equal volume bilateral injections of saline. For 5 days following surgery, animals were given intramuscular (IM) injections of ampicillin (100 mg kg^{-1}).

Induction of Focal Myelitis in Lewis Rats

MOG immunization of lewis rats

Recombinant myelin oligodendrocyte glycoprotein (rMOG) corresponding to the N-terminal sequence of rat MOG (amino acids 1 to 125; Biogen-Idec, Cambridge, MA) was emulsified in incomplete Freund's adjuvant (Sigma-Aldrich) as a 1:1 mixture (Imject IFA; Pierce). About 100 μL (50 μg MOG per rat diluted in saline) of the MOG-IFA emulsion was injected subcutaneously near the base of the tail of each rat at two sites bilaterally (50 μL). The MOG-IFA emulsion was administered 18 days prior to cytokine-ethidium bromide injection.

Stereotaxic injection of cytokine/gliotoxin solution

A small incision was made to expose level T8-T10 of the spinal cord of isoflurane anesthetized animals. Spinal column was stabilized in a stereotactic frame, and a laminectomy was performed on level T9 of the spinal cord. A mixture of cytokines (250 ng of TNF-α, 150 U of INF-γ, and 40 ng of IL-6) and ethidium bromide (1 μg) was injected into dorsal white matter 0.7 mm below the dorsal surface to create a focal area of demyelination.

Electron Microscopy

Rats were transcardially perfused with PBS, followed by perfusion with 4% paraformaldehyde with 1.5% glu-

taraldehyde and 3% sucrose in PBS. Tissue pieces (3 mm^3) were fixed in 1.5% gluteraldehyde with 3% paraformaldehyde, 0.1 M sodium cacodylate and 3 mM $CaCl_2$. Samples were post-fixed in 0.8% potassium ferrocyanide reduced with 1% osmium tetroxide, 0.1 M sodium cacodylate, and 3 mM $CaCl_2$. After a brief dH_2O rinse, samples were embedded in Eponate 12 (Pella), and cured at 60°C for 2 days.

Spinal cord sections (80 nm) corresponding to the site of the lesion were cut on a Riechert Ultracut E with a Diatome diamond knife, collected on formvar-coated 1 × 2 mm^2 copper grids, and stained with uranyl acetate followed by lead citrate. Sections were examined on a Hitachi 7600 transmission electron microscope (TEM) operating at 80 kV. Digital images were captured with an AMT 1 K × 1 K CCD camera. *Rag2/shi* mouse brain tissue was processed as described above except that tissue was post-fixed with phosphate-buffered 4% glutaraldehyde.

Immunosuppresion of Transplanted Focal Myelitis Lewis Rats

Throughout the study all rats (i.e., both cell transplants and saline controls) were subjected to immunosuppression with FK-506 and rapamycin (1 mg kg^{-1} each, LC Laboratories) administered intraperitoneally. Animals were injected daily for the first 6 weeks starting 1 day before cell transplantation. After 6 weeks, drugs were administered every other day.

Behavioral Tests

Hindlimb grip strength was assessed using a Columbus Instruments meter. Readings were acquired in T-peak and measured in pounds of force while animals were supported under their forelimbs with hindlimbs lowered onto the grip bar. Once the animal achieved a stable grip, it was slowly pulled away from the bar. Force was measured only when the animal actively exerted force against the movement. Readings were taken on a weekly basis.

Rota-Rod was used as a measure of motor performance. The speed of the Rota-Rod was increased steadily from 5 to 60 rotations min^{-1} over a 2-min period. The ability of the animal to stay on the Rota-Rod over the two-minute period was recorded. Readings were taken on a weekly basis.

SEP Electrode Implantation, Multi-limb SEP Recording, and Analysis

After anesthetizing the animals with 1% isoflurane, an incision was made at midline and the cranium bone was cleaned. This was followed by implantation of five transcranial screw electrodes (E363/20, Plastics One) on the somatosensory cortex as previously described (All et al., 2009). The electrodes made slight contact with the dura matter without compressing the dura or brain structures. For peripheral simulation of the middle tibial (hindlimbs) or median (forelimbs) nerves needle electrodes (Safelead F-E3-48, Grass-Telefactor, West Warwick, RI) were placed subcutaneously in all four limbs. A constant current stimulator (DS3, Digitimer, Hertfordshire, UK) was used to generate the stimulus pulse (Amplitude 3.5 mA; Pulse width 200 μs; Pulse train frequency 0.25 Hz). Cortical somatosensory evoked potentials (SEPs) were recorded as previously described (All et al., 2009).

Statistical Analysis

Normalized percent change in peak-to-peak amplitude and latency were used as the outcome measures. To examine the statistical differences, Rank Sum Test for comparison between individual limbs from the two groups (cells versus saline) was done with post cell transplantation time points (Day 7–63). To perform the linear trend analysis, the means for the two groups for each limb were fitted with a straight line using SAS PC version 9.1.3 Service Pack 4 (SAS Institute, Cary, NC).

Magnetic Resonance Imaging (MRI)

High resolution *ex vivo* MRI was performed at 4 days after lesion induction to confirm lesion size and location. Prior to imaging, rats were transcardially perfused with PBS followed by 4% paraformaldehyde fixation. Spinal cords were then removed and immersed in Fomblin LC08 (Ausimont USA). *Ex vivo* MR spinal cord images were obtained using a Bruker 500 Mhz spectrometer equipped with a 35-mm diameter transmitter/receiver coil. The 3D spin echo images were acquired with TR = 1,500 ms, TE = 19 ms, matrix = 256 × 256 × 128, FOV = 15 × 10 × 7 mm^3, and four averages.

Histology

Animals were transcardially perfused with PBS followed by 4% paraformaldehyde. The rat spinal cord tissue from level T8-T10 or mouse brain was removed, post-fixed for 24 h in 4% paraformaldehyde, cryopreserved with 30% sucrose solution, and then flash frozen. 30-μm thick axial tissue sections were cut on a cryostat and slides processed for hematoxylin/eosin, eriochrome, and immunofluorescent staining.

Immunofluorescence and Cell Counting

Primary antibodies and dilutions used in this study were: Human Nuclei (1:250, MAB1281, Millipore, Billerica, MA); Olig-2 (1:500, AB9610; Millipore, Billerica, MA) Glial fibrillary acidic protein (GFAP) (1:500, Z0334 DAKO, Carpinteria, CA); Myelin basic protein (MBP) (1:500, MCA409S; AbD Serotec; Kidlington, Oxford). A2B5 (MAB1416, R&D Systems), PDGFRalpha (MAB1264, R&D Systems), Nestin

(MAB5326, Millipore), PSA-NCAM (MAB5324, Millipore), CD68 (#M0718, DakoCytomation), PECAM (CBL468, Millipore), IBA-1 (1:250, Wako Chemicals Richmond, VA).

The different combinations of primary antibodies were detected by immunofluorescence using goat anti-rabbit, goat anti-rat, and anti-mouse IgG coupled to Alexa Fluor-488 (green), Alexa Fluor-350 (Blue), and Alexa Fluor-594 (red) (1:200, Molecular Probes).

Cell counts were done either manually or with Nikon NIS-Elements Imaging Software. For each animal, 8–10 sections (30 μm thickness) around the lesion were stained for human nuclear antigen (HuNA) and the total number of positive nuclei were counted. The total number of surviving hGRPs was computed as an approximation of the integral of number of cells with respect to distance from the most rostral spinal cord section containing HuNA+ cells, using trapezoidal integration in Matlab 7.5 (The Mathworks, Natick, MA).

RESULTS

Phenotypic Features of hGRPs Before Transplantation

In vitro immunocytochemical characterization of the hGRPs was performed using a panel of antibodies representing antigens expressed by the potential cellular phenotypes present within each preparation (hGRPs: A2B5, PDGFRa, and nestin; astrocytes: GFAP; neurons and neural precursors: PSA-NCAM; microglia: CD68; and endothelial cells: PECAM). The percentage of total cells positive for these antigens was quantified on nine preparations documenting the presence of desirable markers (A2B5, 82.8% ± 7.8%; PDGFRalpha, 91.5% ± 6.6%; GFAP, 70.3% ± 11.6%; and nestin, 86.9% ± 6.1%), and low levels of unintended cellular phenotypes (CD68, 0.6% ± 0.7%; PECAM, 0.6% ± 1.1%; and PSA-NCAM, 3.4% ± 1.4%). The cells used for transplantation in these studies fell within these specifications.

hGRPs Transplantated into Neonatal Myelin-Deficient Immuno-Deficient Mouse Brain Proliferate, Migrate, and Extensively Myelinate Axons

To probe the differentiation and myelination potential of hGRP cells in developing brain, cells were transplanted into the lateral ventricle of neonatal (P1) immune deficient *rag2*$^{-/-}$ myelin-deficient *shi*/*shi* mouse brain. Double immunohistochemistry for human nuclei (anti-human nuclear antigen antibody: HuNA) and cell-type specific markers (GFAP, MBP, and Olig2) was performed to assess cell distribution and differentiation. Analysis of tissue samples at 2 weeks after transplantation revealed cells mainly within or in the vicinity of the lateral ventricle of the brain (Fig. 1A). At this time point, the number of HuNA positive cells was relatively low suggesting a significant initial loss of grafted cells. Very few transplanted cells were positive for the OPC marker Olig2 (Fig. 1A), GFAP^{+} astrocytes were observed rarely (Fig. 1B, arrowhead), and myelin basic protein (MBP) expression was not detected (Fig. 1C).

Six weeks after transplantation, cells had proliferated considerably and were found bilaterally in the brain structures surrounding the lateral ventricles, including the corpus callosum, striatum, and hippocampus. There was a marked preference for cells to localize and migrate within the white matter. Six weeks after transplantation was the earliest sampling point when hGRPs stained positive for MBP and developed branched oligodendrocyte-like morphology. Notably, with many human cells present in the brain, only few stained positive for MBP (Fig. 1F) and GFAP (Fig. 1E, arrowhead). A significant fraction expressed Olig2 (Fig. 1D).

Over time there was an apparent increase in cell number and dispersion throughout the brain; at 13 weeks after transplantation, cells could be found in most brain structures from olfactory bulb to cerebellum. Importantly, the extent of myelination escalated and at 13 weeks certain brain structures, i.e., the corpus callosum and fimbria, showed extensive positivity for MBP (Fig. 1I). Many xenograft-derived cells remained positive for Olig2 (Fig. 1G), while astrocytic progeny, as determined by GFAP reactivity, was rare and found mostly within gray matter (Fig. 1H). Electron microscopic analysis of *Rag2*/*shi* mouse brain tissue 14 weeks after transplantation revealed that many axons, particularly within the corpus callosum, were surrounded by compact, multilamellar myelin consisting of ~9–10 layers, indicating proper formation of myelin (Fig. 1J,K). Transplant-derived myelin was clearly identifiable from host myelin having only a few loosely structured lamellae (Fig. 1L,M).

hGRPs Transplanted into Adult Focally Demyelinated Rat Spinal Cord Survive, Migrate, and Enter the Olig2+ OPC Stage

Animal *model* of focal inflammatory demyelinated lesions

To probe the ability of hGRPs to remyelinate demyelinated axons, we induced a focal demyelinated lesion in the spinal cord of Lewis rats. The rat model is based on the model published by Kerschensteiner et al. (2004), with a modification (see Materials and Methods) that more robustly induces clinical and histological evidence of focal inflammatory demyelination. Lesions were created within the dorsal funiculus of spinal cord at the T9 level (Fig. 2A). Using this model, we achieved a substantial, long-lasting functional deficit as demonstrated by Rota-Rod test (Fig. 2J). Mild deficits were observed 24 h after injection that gradually increased to reach a maximum at 3–5 days after lesioning. Grip strength assessment, which probes primarily motor function, showed a substantial spontaneous recovery with values returning to baseline at about 40 days after lesion induction (Fig. 2K). In T2-weighted MRI at 4 days after induction, lesions appeared as hyperintense regions, mainly limited

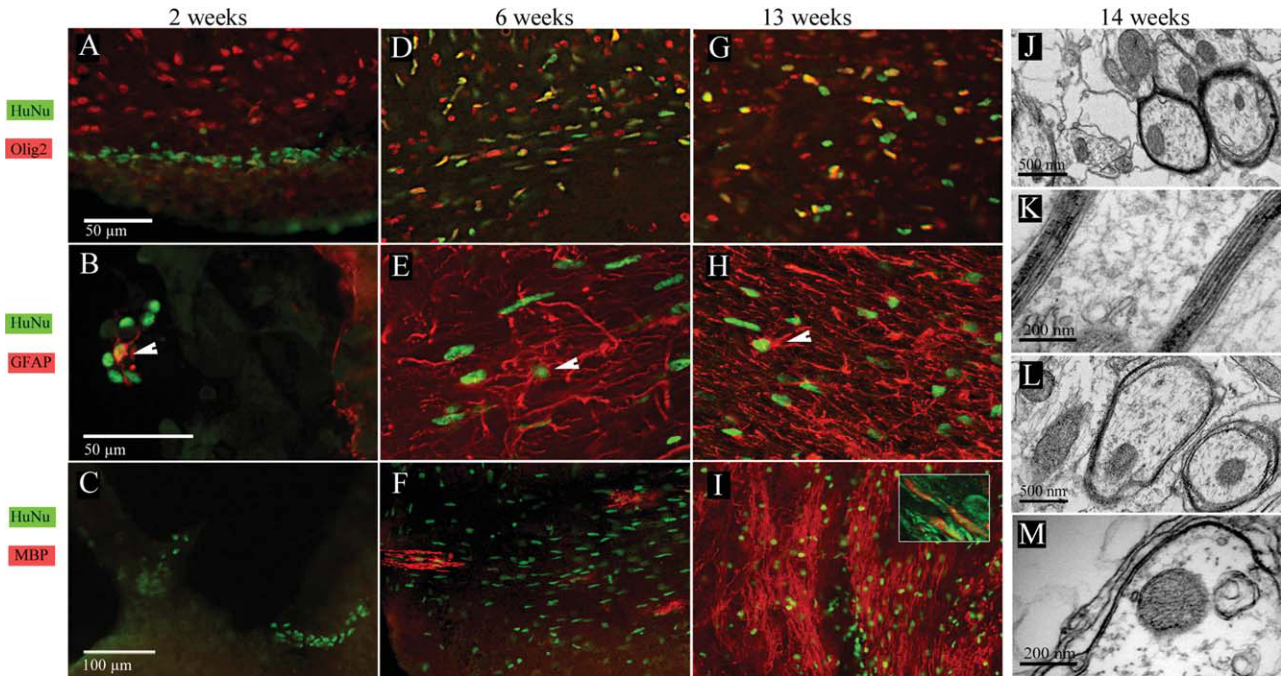

Fig. 1. Phenotype of hGRPs transplanted into myelin-deficient, immunodeficient mouse brain. (**A**–**C**) Two weeks after ICV transplantation, HuNA-positive hGRPs were found within or near the vicinity of the lateral ventricle. Occasionally, grafted cells co-localized with the Olig2 marker (A) or GFAP (B). MBP expression at this time was not detected (C). (**D**–**F**) Six weeks after transplantation, hGRPs substantially expand and were found in brain structures relatively close to the ventricles. A large proportion of the cells expressed Olig2 (D) and some of those residing within gray matter were positive for GFAP (E, arrowhead). At this time, the first MBP-positive oligodendrocytes could be observed (F). (**G**–**I**) Thirteen weeks after grafting, many hGRPs co-express the Olig2 marker (G), with those positive for GFAP presenting a more mature astroglial morphology (H). At this point, MBP expression and myelination in some brain structures was very robust (I) High resolution confocal microscopy (I, inset) demonstrates that MBP myelin (red) surrounds TuJ1 axons (green). (**J**–**M**) electron microscopy 14 weeks after cell transplantation revealed that many axons within corpus callosum were surrounded by thick myelin sheaths (J). High magnification images clearly demonstrate a normal myelin structure with multiple layers of compact myelin and dense lines present (K). Numerous axons exhibited a myelin structure typical for the shiverer phenotype with only a few loosely organized lamellae (L,M).

to dorsal white matter spanning over 7 mm rostro-caudally (Fig. 2B,C). Histologically, at 2–3 weeks lesions were largely confined to dorsal white matter, appeared hypercellular as assessed by H&E staining (Fig. 2D), and fully demyelinated as assessed by Eriochrome staining (Fig. 2E). The region was highly positive for activated microglia (IBA-1$^+$; Fig. 2F). Silver staining demonstrated that while axonal density was decreased in the core of the lesion, many axons were preserved (Fig. 2G). This finding was confirmed by electron microscopy, which showed many demyelinated axons with preserved axonal integrity within the lesion (Fig. 2H).

The presence of naked but viable axons validates the utility of our model for evaluating the efficacy and remyelination potential of hGRP therapy for treatment of demyelinated lesions present in TM and MS.

Cell transplantation, survival, and migration

One week after lesion induction, hGRPs (4×10^5 cells) were stereotaxically transplanted into the epicenter of the demyelinated dorsal funiculus lesion of rat spinal cord. Animals were sacrificed and spinal cord tissue was collected at 3, 7, and 14 weeks after transplantation. Consistent with observations in mouse experiments, cells were found predominantly near the injection site at the earliest time point (3-week post-grafting) (Fig. 3A), with very modest rostro-caudal migration (hGRPs populated only about 5% of the lesion length) (Fig. 3E). Seven weeks post-grafting cells markedly expanded and their migration both axial and rostro-caudal was much more pronounced; hGRPs then populated about 70% of the lesion length (Fig. 3B,F). Cells continued to migrate and expand, and populated the entire lesion by 14-week post-transplantation (Fig. 3C,G). While the cell distribution was not limited to the lesion, a preference of hGRP progeny to accumulate within the lesion was noted. Quantitative analysis of HuNA positive cell numbers in tissue samples from 3-, 7,- and 14-week post-transplantation was consistent with an initial reduction in number of surviving human cells 3 weeks after transplantation. The initial decrease is followed by a gradual increase to ~10-fold over the injected cell number at 14 weeks. This suggests that the cells divided four to five times over the time course of the experiment.

Phenotypic features of hGRPs after transplantation into *demyelinated* rat spinal cord

Immunohistochemical analysis at 3 weeks after transplantation revealed that 20% of xenograft-derived cells were Olig2 positive (Fig. 4A). Although precise co-localization of nuclear HuNA and GFAP or MBP staining was often difficult to detect in the background of endogenous immunoreactive cells, it was possible with the aid of confocal

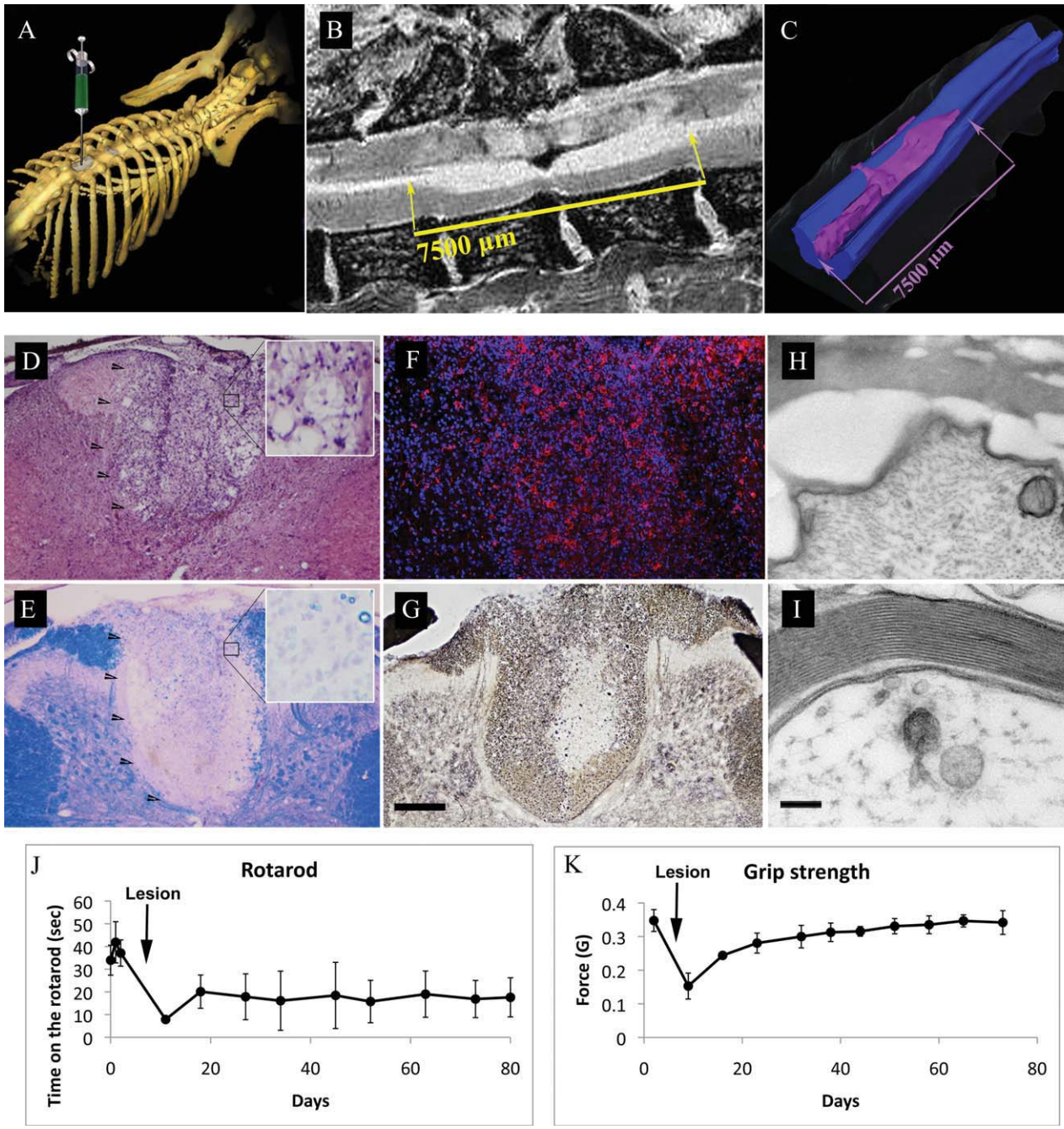

Fig. 2. Focal inflammatory/gliotoxic demyelination of rat thoracic spinal cord. (**A**) Diagram showing the site of laminectomy and the induction of focal demyelination at the T9 level. (**B**) T2-weighted sagittal MRI scan of rat spinal cord showing the extent of the lesion. Hyperintense demyelinated area extends rostro-caudally for about 7.5 mm. (**C**) Segmentation and surface rendering of the MRI scan demonstrates the location and full distribution of the lesion and is confined to the dorsal white matter. (**D–I**) Histological characterization of demyelinating lesion. (D) H/E staining demonstrates an area of increased cellular density within the dorsal white matter. (E) Eriochrome staining shows complete demyelination within the lesion. (F) Immunofluoresence localization of the IBA-1 antigen (red) reveals extensive infiltration of the lesion by activated microglia. (G) Silver stain delineates axonal density and shows an area of axonal loss in the core of the lesion; scale bar for D–G = 200 μm. (H,I) Electron microscopy of the lesioned site (H) shows loss of dense lines and separation of myelin from axolemma. (I) Normal axon in the ventral white matter; scale bar = 100 nm. (**J**,**K**) Behavioral assessment of neurological function. (J) Rotarod test results show that performance after lesion induction was reduced to about 25% of baseline, was followed by minor recovery, and stabilized at 50% of the baseline level. (K) Grip strength test showed a similar reduction in test scores following the lesion induction, but recovery was much greater and the values returned to baseline at about 40-day post-lesion induction.

microscopy to identify many examples of human cells expressing GFAP (Fig. 4B). At this time point, hGRP progeny appeared MBP negative (Fig. 4C). Seven weeks after transplantation, the total number of xenografted cells increased, with a similar fraction (17% ± 4%) expressing Olig2 (Fig. 4D). Similarly, at this time point a significant fraction co-localized with GFAP (Fig. 4E) and there was no evidence of MBP/HuNA colocalization (Fig. 4F). At the lat-

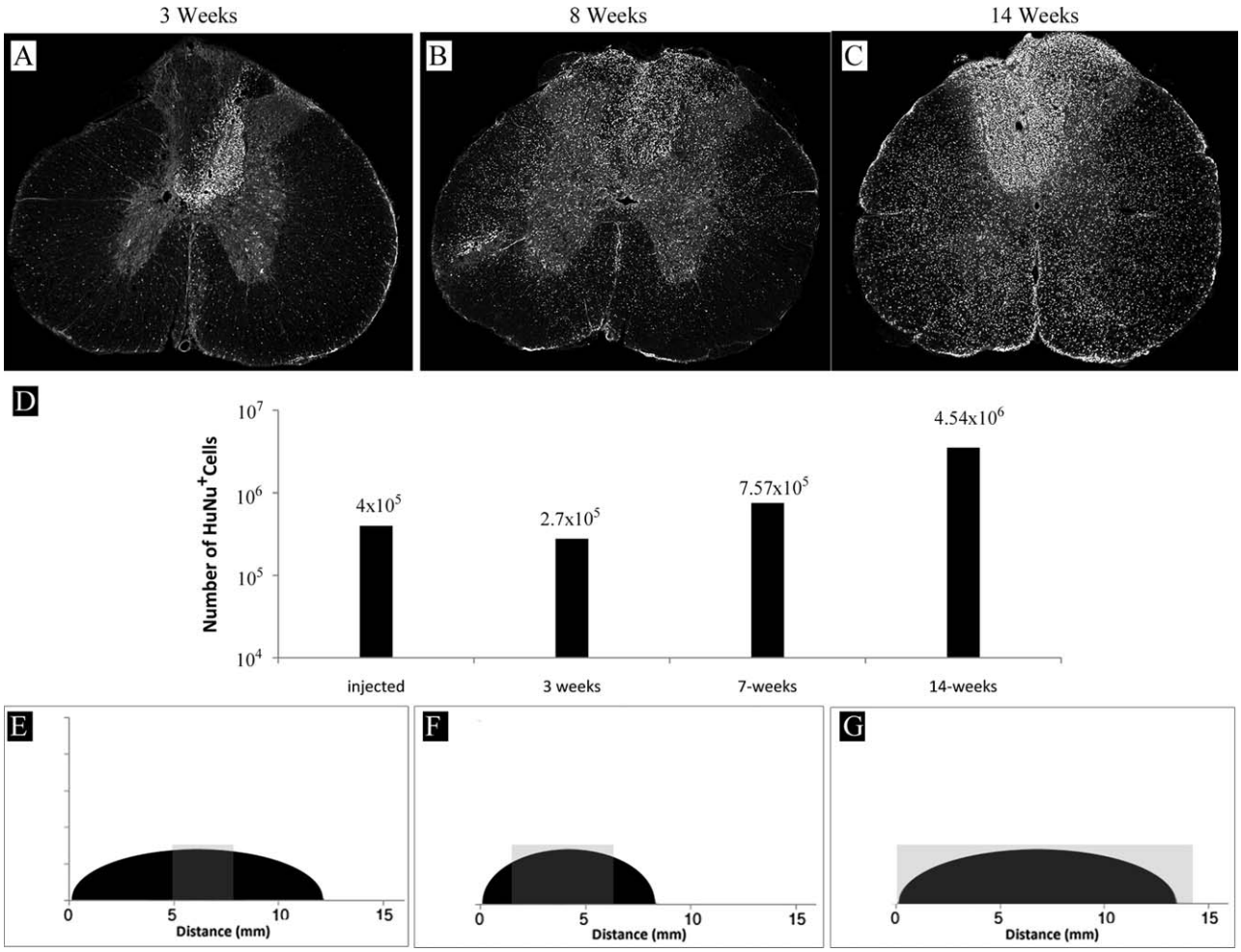

Fig. 3. Survival, expansion, and migration of hGRPs transplanted into rat spinal cord. (**A**) Three weeks after transplantation, hGRPs, as detected by HuNA immunostaining (white), were found mostly within the injection site, with few cells migrating into the surrounding spinal cord tissue. (**B**) Eight weeks after injection, cells amplified and migrated quite extensively. (**C**) Fourteen weeks after transplantation, the number of cells substantially increased and their migration was remarkable. (**D**) Graph represents HuNA-positive cell quantification and shows that the number of hGRPs initially dropped and the cells gradually expanded over time, undergoing four to five cell divisions over the period of 14 weeks. (**E–G**) Graphs show rostral-caudal extent of the demyelinating lesion (black area) as well as localization of $HuNA^+$ cells (gray area). (E) Three weeks after transplantation, human cells were found in sections spanning over 3 mm. (F) Eight weeks after transplantation cells extended rostral-caudal with a total migration distance over 8 mm; at the 14 weeks time point (G) the distance had grown to over 15 mm. The entire rostral-caudal span of the lesion was populated by hGRPs at this time point.

est time point (14-week post-grafting), 3.8% ± 3.62% hGRP progeny residing within the core of the lesion were Olig2 positive (Fig. 4G). At this time, there were very few examples of MBP/HuNA colocalization (Fig. 4I, arrowhead), and many human cells stained positive for GFAP (Fig. 4H, arrowheads). Triple immunostaining for GFAP, Olig2, and HuNA showed that co-localization of these markers was very rare; example of such co-localization is shown in Fig. 4G (inset).

Behavioral and Electrophysiological Assessment of Neurological Function Following hGRPs Transplantation into Focally Demyelinated Rat Spinal Cord

Behavioral tests and electrophysiological measurements were performed prior to lesion to obtain baseline values. Additional measurements were performed in the interval between lesion induction and transplantation. At that time all animals presented various degrees of neurological deficits including mild hindlimb paresis and some movement discoordination. Rota-Rod and hindlimb grip strength test scores reflected these observations, and the scores were substantially reduced as compared with pre-lesion status (Fig. 5A,B). Animals were divided into experimental groups while randomizing for the level of disability such that the mean values of behavioral scores was approximately the same for the cell transplantation ($n = 16$) and saline control ($n = 14$) groups. Weekly behavioral testing after transplantation for a period of 95 days did not reveal significant differences between hGRP transplant and saline groups (Fig. 5A,B).

Electrophysiological measurements of somatosensory evoked potentials (SEP) were performed (prelesion baseline, post-lesion, post-transplant, and weekly thereafter)

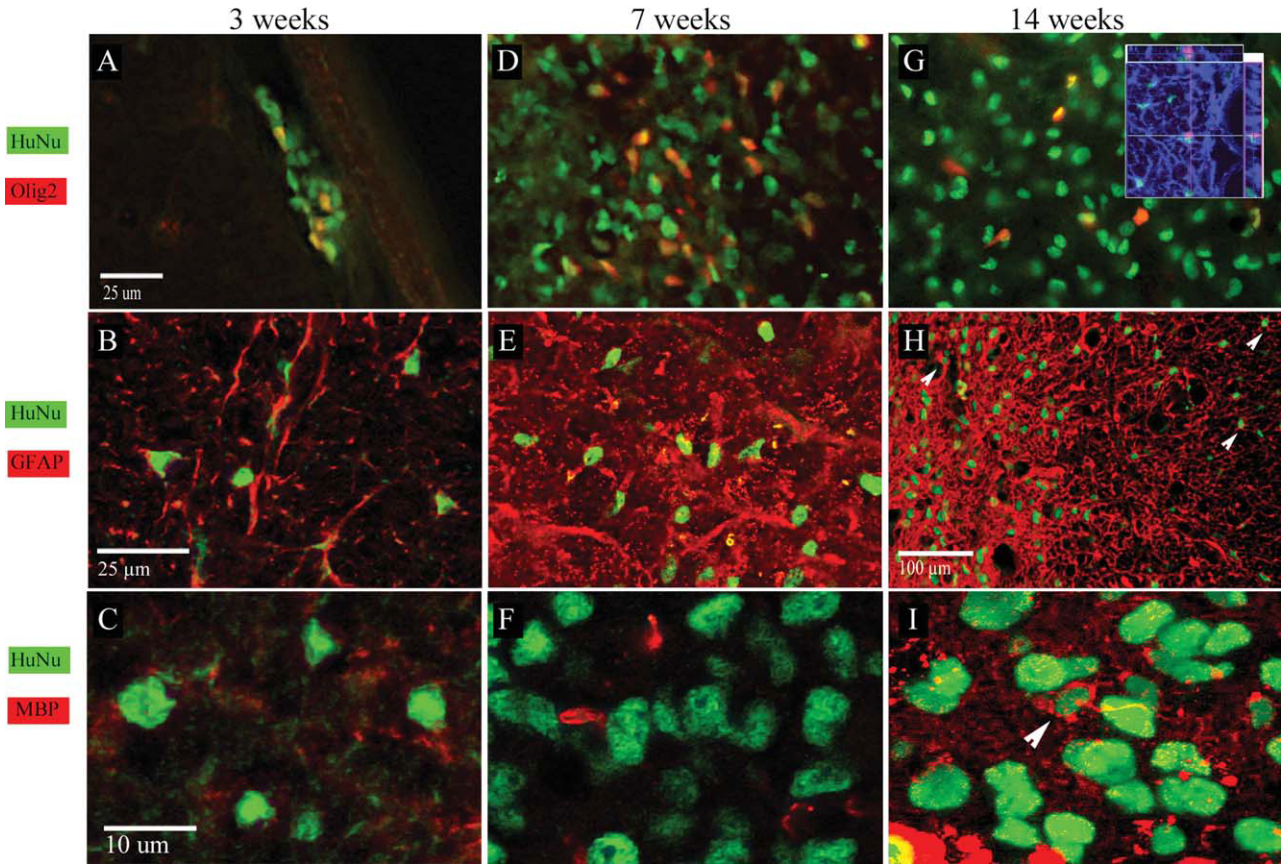

Fig. 4. Phenotype of hGRPs transplanted into focally demyelinated rat spinal cord. (**A–C**) Three weeks after tranplantation, many of hGRPs co-localized with the Olig2 marker (A). Co-expression of HuNA and GFAP was quite frequent (B). MBP expression at this time was not detected (C). (**D–F**) Seven weeks after transplantation, 17% ± 4% of hGRPs expressed Olig2 (D), and many were GFAP positive (E). No MBP expression in hGRPs was detected (F). (**G–I**) Fourteen weeks after grafting, 3.8% ± 3.62% of hGRPs co-expressed Olig2 (G), and a large proportion was GFAP positive (H, arrowheads). Inset in G shows triple immunostaining for GFAP (blue) Olig2 (magenta) and HuNA (green). A rare example of a cell expressing all three markers is shown with the orthogonal view. At this time point, single MBP-expressing human cells were detected within the lesion, which represented 0.68% ± 1% of total hGRPs (I).

and N1 peak latencies were statistically compared. SEP recorded with stimulation from forelimbs showed no significant variation in peak latencies compared with baseline values in both groups (not shown). This is expected, since the injury at T8 primarily affects the hindlimbs.

Hindlimb SEPs for the saline group showed a mean upward trend in latency over 9 weeks, indicating a slowing of somatosensory response, while the hGRP group showed a mean downward trend indicating an improvement in conduction (Fig. 5C,D). These results indicate a benefit of hGRP transplants compared with saline injections over a period of 9 weeks after transplantation. Statistical analysis by a non-parametric Mann-Whitney Rank sum test for N1 latency values post-transplantation showed a significant difference between the left hind limbs ($P < 0.001$). While the number of animals analyzed at the last few time points is small ($n = 2$ for saline and $n = 3$ for hGRPs), we believe the qualitative comparative analysis in this study provides insight into the hurdles that exist in achieving a successful functional improvement for cell therapy in inflammatory demyelinating CNS disorders.

Histological Analysis of Demyelinated Lesion in the Spinal Cord of GRP Transplanted and Control Rats

Immunostaining for astrocytes (GFAP), total microglia (IBA-1), and activated microglia (ED-1) 14 weeks after cell injection (15 weeks after lesion induction) revealed an increased number of microglia within the lesion of both transplanted and control animals (Fig. 6A,B). While the amount of activated ED-1 positive cells was comparable between the groups (Fig. 6A,B, red), there was a substantially higher amount of total microglia (IBA-1+) in the cell transplant group (Fig. 6A,B, green). Interestingly, immunostaining for astrocytes (GFAP+) showed a pronounced difference between transplanted and control spinal cord lesions; entire lesions were highly positive for GFAP in cell-transplanted rats, (Fig. 6C, red) while only the periphery of the lesion was strongly GFAP positive in control rats (Fig. 6D, red). This suggests that transplanted GRPs contributed significantly to astrocytosis within the lesion and, given the improvement of electrophysiological function, may

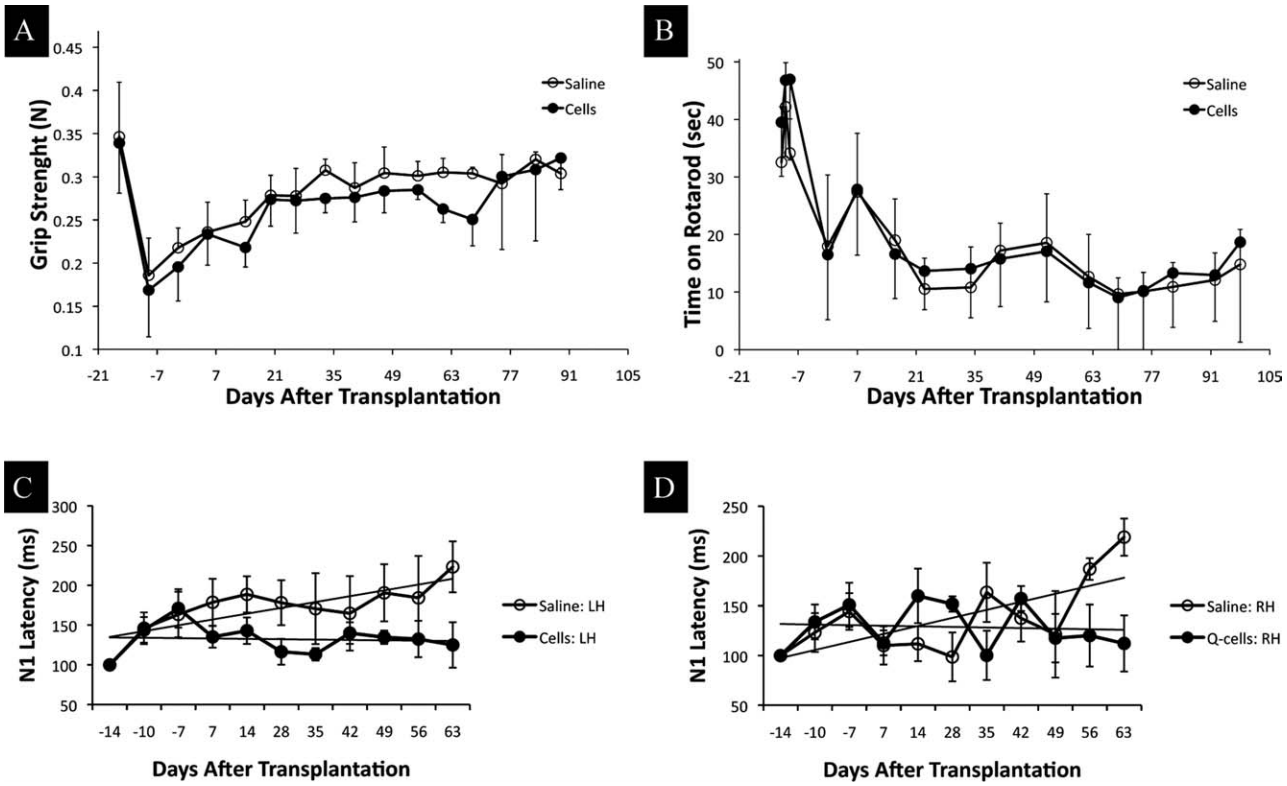

Fig. 5. Behavioral and electrophysiological assessment of neuronal function following hGRP transplantation into demyelinated rat spinal cord. (**A**) Grip strength assessment scores were substantially reduced in both the cell transplantation and control groups after the lesion. Over the time period of the experiment, both groups gradually improved without statistically significant differences. (**B**) Rotarod test scores were reduced after lesion induction, and remained at a low level throughout the experiment. There were no significant differences between the groups. (**C**, **D**) Normalized changes in N1 peak latencies with the two panels showing latencies for SEPs with stimulation from two hindlimbs (Panel C—left hindlimb; Panel D—right hindlimb). In both limbs, the saline cohort (open circles) shows a mean upward trend indicating slowing of the somatosensory response; the hGRP cohort (filled circles) shows a slight downward trend, indicating improvement of conduction speed. The mean trends were significantly different for the left hindlimb (A) $P < 0.001$.

have a protective or regenerative effect for axons located within the lesion.

DISCUSSION

The rationale for using cell transplantation for treatment of demyelination derives from the observation that, in MS lesions, endogenous OPCs initially engage in remyelination (Chang et al., 2000), but over time, the number of OPCs in the lesions decline and remyelination becomes inefficient (Raine, 1997). Transplantation of exogenous precursors capable of forming myelinating oligodendrocytes is an attractive approach with the potential to salvage denuded axons and improve the prospects of TM and MS patients. One of the first demonstrations of the myelinating potential of human OPCs is the use of human fetal CNS fragments transplanted into the dysmyelinated shiverer mouse brain (Gumpel et al., 1987). However, the use of fetal tissue fragments is not optimal from a clinical perspective, because the material is inherently difficult to standardize due to its complex and heterogeneous nature. With the discovery of several markers specific to glial precursor cells, including NG2, Olig2, or surface marker A2B5, it is possible to identify, and purify, populations of cells that are precursors for oligodendrocytes and astrocytes. Other potential sources of neural precursors with myelinating potential include human embryonic stem cells (hESCs) and iPS cells. Protocols are being developed that induce differentiation of these pluripotent cells into glial precursors suitable for transplantation. While functional benefits of hESC-derived precursors in a model of spinal cord injury have been demonstrated (Keirstead et al., 2005), it is presently not clear which source of precursor will display the greatest potential for repairing demyelinated lesions.

This study reports on the first application of hGRPs in an adult focally demyelinated rat host. For purposes of comparison, hGRPs were also implanted into perinatal, immune-deficient, and dysmyelinated mouse brain. Our focally demyelinated rat spinal cord model represents a focal autoimmune encephalomyelitis (Kerschensteiner et al., 2004), and includes administration of a gliotoxic compound (ethidium bromide) to achieve a more robust and consistent phenotype; this closely resembles the neural tissue environment found in patients affected by TM and MS. Immunosuppressive treatment with Rapamycin and FK506 after autoimmune induction provided long-term protection of the human xenograft. Because of the lack of compact myelin and no endogenous immunodetectable myelin basic protein, the dysmyelinated shiv-

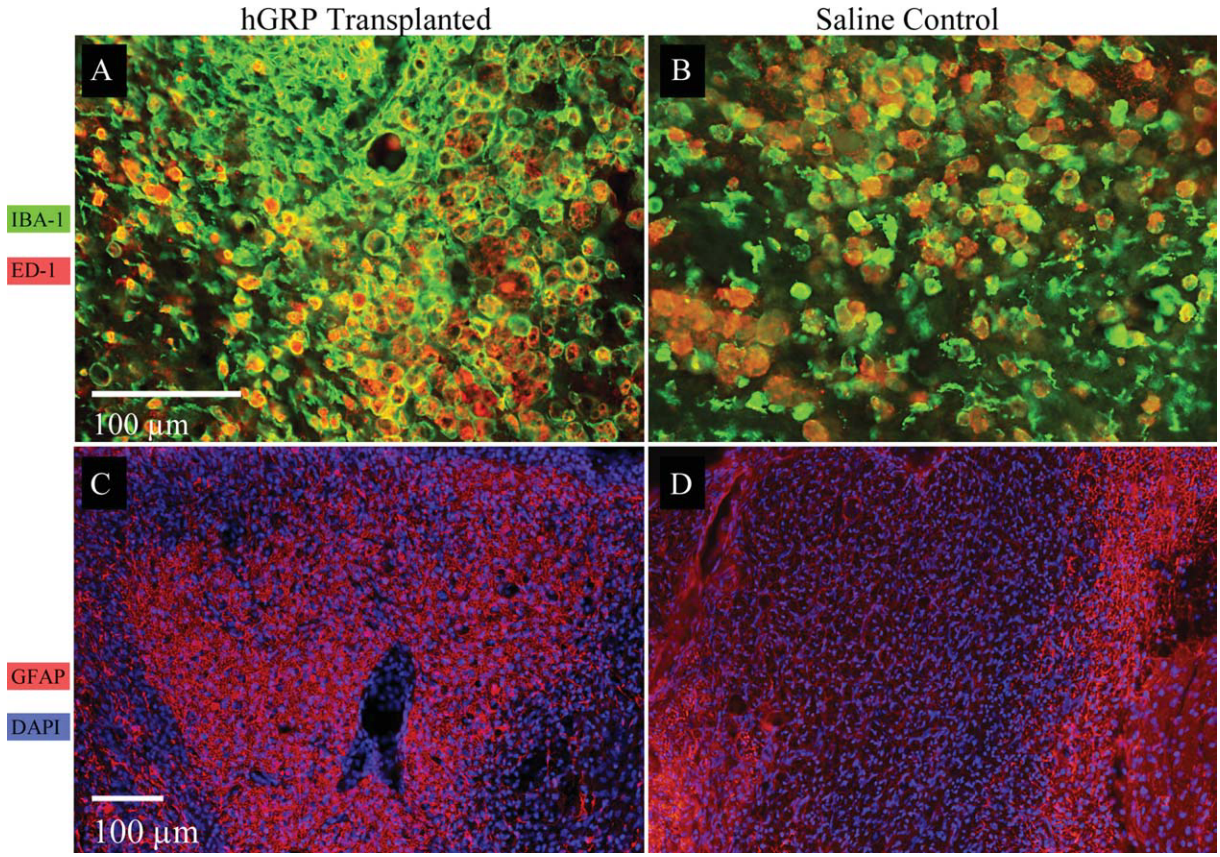

Fig. 6. Histological analysis of demyelinated lesion 14 weeks after hGRP transplantation. (**A**, **B**) Immunostaining for microglia IBA-1 (green), and ED-1 (red), in spinal cord lesion of rats transplanted with hGRP cells (A) or saline controls (B). Increased presence of total microglia (IBA-1) as well as activated microglia (ED-1) is observed in both groups, with greater numbers found in hGRP transplanted rats. (**C**, **D**) Immunostaining for astrocytes GFAP (red), and DAPI (blue), in transplanted (C) vs. control rats (D). hGRP-transplanted animals show much stronger staining within the lesion.

erer mouse model allows for rigorous evaluation and quantification of transplant-derived myelin, while the Rag2 background of the double mutant mice enables graft evaluation without the interference of immune rejection, inflammation, or differentiation disruption caused by immunosuppressive treatment.

Estimating the Number of Cells Needed for Effective Remyelination

For effective repair of extensive demyelination, OPCs must populate the lesion with myelinating oligodendrocytes. In the case of transplantation of exogenous progenitors, several factors will determine the number of cells required to achieve tissue regeneration, in particular the minimum number of mature oligodendrocytes that are required, and the survival, expansion and rate of differentiation of progenitor cells into myelinating oligodendrocytes. Based on the literature, the number of mature oligodendrocytes within the white matter of the spinal cord ranges between 400 and 500/mm^3 (Beattie et al., 2002). With an assumption that grafted cells may have a reduced arborization ability [i.e., xenograft-derived oligodendrocyte can myelinate 1–6 axons whereas endogenous oligodendrocytes myelinate 10–60 axons (Baumann and Pham-Dinh, 2001; Murray and Blakemore, 1980)], we estimate that 4–5 $\times$ 10^3/mm^3 graft-derived oligodendrocytes would be sufficient to fully repair a 1 mm^3 demyelinated lesion. Our rat model of focal inflammatory demyelination displays lesions that spread rostro-caudally for up to 7.5 mm, and 1 mm dorso-ventrally and 1 mm medio-laterally (Fig. 2B,C). Thus, the volume of demyelination reached ~7 mm^3 which, based upon the above considerations, would require 2.8–3.5 $\times$ 10^4 graft derived myelinating oligodendrocytes for complete repair. In this study, 4 $\times$ 10^5 cells were injected directly into the center of the lesion, were immunoprotected by FK506 and rapamycin, distributed throughout the lesion (Fig. 3E), and survived exceptionally (~4.54 $\times$ 10^6 graft-derived cells at 14 weeks after transplantation) (Fig. 3D). This number exceeds by 100-fold the previously estimated 2.8–3.5 $\times$ 10^4 number of myelinating oligodendrocytes required to repair a focal lesion of about 7 mm^3, and is consistent with the feasibility of remyelination by exogenous progenitor transplantation, given the distribution (both within and outside of the lesion) and differentiation (albeit a minor population of graft-derived MBP-positive oligodendrocytes) of graft derived cells.

Successful Engraftment Following Intraparenchymal Cell Injection Highly Depends on Robust Cell Migration

For multifocal CNS lesions, intracerebroventricular (ICV) or systemic cell delivery is being considered (Einstein et al., 2007; Janowski et al., 2010; Walczak et al., 2007, 2008) as the most effective administration route; while direct delivery in the proximity of the lesion remains the method of choice for localized lesions (Mothe and Tator, 2008). With this latter approach, injected cells initially occupy a small area in the region of the injection site (see Fig. 3A), and their ability to migrate to all portions of the lesion is of paramount importance for the success of a cell-based therapy. As demonstrated in this study, hGRPs have an exceptional ability to disseminate in both the developing mouse brain and in the adult rat spinal cord. Within 14 weeks of the spinal cord transplantation experiment, hGRPs were able to migrate and populate lesions spanning rostrocaudally for over 7 mm. The propensity of the xenografted cells to preferentially populate the lesion may be due to an inherent tropism of GRPs toward a lesion environment. Alternatively, the lesion environment may be a permissive substrate for GRP survival, expansion and migration, or non-lesion surrounding tissue may be relatively inhibitory for such behaviors. While further studies will be required to differentiate these possibilities, our results document migratory capabilities of hGRPs sufficient to distribute within relatively large lesions. However, in some clinical cases of TM, the lesion length extends to as much as the entire spinal cord (Krishnan et al., 2006), and, in these cases, injection of the cells at multiple levels would be required.

Differentiation of hGRPs-Dynamics and Factors Potentially Inhibiting Oligodendrocyte Maturation and Myelination

The ability of transplanted progenitor cells to differentiate and functionally integrate *in vivo* is a prerequisite for, and surrogate measure of, therapeutic potential. The timing of progenitor cell maturation is also important and should be considered prior to clinical application of cell-based therapy for de- or dys-myelinating disorders. This study provides evidence for the robust myelinating capabilities of hGRPs transplanted into the dysmyelinated, developing mouse brain. We found that, in this environment, myelination is initiated between two and six weeks after transplantation with extensive myelination after three months: consistent with a previous report (Windrem et al., 2008). Electron microscopy 14 weeks after cell transplantation revealed that many axons within the corpus callosum were surrounded by compact myelin sheaths (Fig. 1J,K). The thickness of the myelin at this time point was 9–10 layers, which is significantly more than the 3–4 endogenous layers typically found in shiverer brain. Numerous axons exhibited a myelin structure typical for the shiverer phenotype with only a few loosely organized lamellae (Fig. 1L,M), indicating that at 14 weeks myelination by transplanted cells was only partial. As shown by Windrem et al. myelination by hGRPs progresses and at 1 year after transplantation is more complete. However, in another study myelinating cells were observed 17 days after grafting human embryonic brain tissue fragments into neonatal shiverer mice (Gumpel et al., 1987). Even faster myelination was reported with the use of rodent cells; adult rat spinal cord neural stem/progenitors cells expressed MBP in the adult dysmyelinated mouse spinal cord one week after transplantation (Mothe and Tator, 2008). These studies indicate that the time required for maturation varies widely, likely depending on several factors: species of the engrafted cells (human vs. rodents), context of the transplant (allograft vs. xenograft; neonate vs. adult recipient), or stage of differentiation/maturation of the graft cells at the time of transplant.

In contrast to the dysmyelinated mouse brain, hGRPs transplanted into focally demyelinated rat spinal cord differentiated mainly into GFAP-positive astrocytes. Several factors may explain this observation. First, an impact of the local tissue environment upon differentiation potential has been seen with the use of rat spinal cord-derived neural stem cells, which become myelinating oligodendrocytes in dysmyelinated mouse spinal cord, and Schwann-like cells in focal lesions induced by ethidium bromide (Mothe and Tator, 2008). Second, it has been reported that elimination of astrocytes as a result of ethidium bromide-induced demyelination has a negative effect on remyelination by endogenous OPCs (Talbott et al., 2005), as well as transplanted OPCs (Talbott et al., 2006), though this negative effect was alleviated through co-transplantation of OPCs and astrocytes (Talbott et al., 2006). Third, inflammation caused by the inclusion of a MOG/cytokine component in the focal demyelination model may influence the ability of the cells to myelinate; however, it has been shown that inflammation has a promyelination effect in retinal transplants of OPCs (Setzu et al., 2006). Finally, in our experiments, xenografts were immunoprotected with the use of FK 506 and rapamycin. It has been reported that when mTOR signaling was inhibited by rapamycin, oligodendrocyte differentiation and myelination was reduced both *in vitro* (Tyler et al., 2009) and *in vivo* (Narayanan et al., 2009). The potential interplay between host environment and immune suppression protocols on the fate of hGRP transplants thus warrants further study.

Although efficient differentiation into a MBP-positive phenotype was not observed, physiological benefits were documented. While hGRPs can directly form myelinating oligodendrocytes, their remyelinating potential may not be restricted to this capability: transplanted cell progeny could alter the host environment in ways which promote endogenous remyelination. Astrocytes secrete a wide variety of trophic and neuroprotective factors (Abbott et al., 2006); supportive factors are known to preserve motor function, protect oligodendrocytes from a broad range of pathological insults, and promote remyelination from endogenous oligodendrocytes (Iannotti et al., 2003).

The lack of behavioral improvement following electrophysiological function sparing may have been due to the

time frame studied or the relative insensitivity of behavioral assays. Goldman and coworkers (Windrem et al., 2008) reported electrophysiological improvement under non-inflammatory conditions 12 months after transplantation: considerably longer than the 14-week duration of the present study. Notably, 3.8% of our transplant-derived cells were Olig2-positive at the longest time point, suggesting the persistence of OPCs still capable of becoming mature oligodendrocytes. A delayed wave of myelination by remaining human Olig2$^+$ precursor cells could be necessary for behaviorally observable benefits.

In summary, we have demonstrated that hGRPs are a promising candidate for cell therapy of myelin disease as they have remarkable migratory abilities, preferentially populate demyelinated lesions, can expand *in vivo*, and do not form tumors. The capacity of these cells to myelinate depends on the local environment, and, while the developing brain allows for full realization of their developmental process, focally demyelinated adult rat spinal cord is much more complex and requires more study to characterize factors that inhibit and promote the myelination potential necessary to achieve functional benefit for patients.

ACKNOWLEDGMENTS

The authors thank Mary McAlister for editorial assistance and Cynthia Levinthal for preparing the samples used for EM analysis.

REFERENCES

Abbott NJ, Ronnback L, Hansson E. 2006. Astrocyte-endothelial interactions at the blood-brain barrier. Nat Rev Neurosci 7:41–53.

All AH, Walczak P, Agrawal G, Gorelik M, Lee C, Thakor NV, Bulte JW, Kerr DA. 2009. Effect of MOG sensitization on somatosensory evoked potential in Lewis rats. J Neurol Sci 284:81–89.

Baumann N, Pham-Dinh D. 2001. Biology of oligodendrocyte and myelin in the mammalian central nervous system. Physiol Rev 81:871–927.

Beattie MS, Harrington AW, Lee R, Kim JY, Boyce SL, Longo FM, Bresnahan JC, Hempstead BL, Yoon SO. 2002. ProNGF induces p75-mediated death of oligodendrocytes following spinal cord injury. Neuron 36:375–386.

Chang A, Nishiyama A, Peterson J, Prineas J, Trapp BD. 2000. NG2-positive oligodendrocyte progenitor cells in adult human brain and multiple sclerosis lesions. J Neurosci 20:6404–6412.

Einstein O, Fainstein N, Vaknin I, Mizrachi-Kol R, Reihartz E, Grigoriadis N, Lavon I, Baniyash M, Lassmann H, Ben-Hur T. 2007. Neural precursors attenuate autoimmune encephalomyelitis by peripheral immunosuppression. Ann Neurol 61:209–218.

Goldman S. 2005. Stem and progenitor cell-based therapy of the human central nervous system. Nat Biotechnol 23:862–871.

Gregori N, Proschel C, Noble M, Mayer-Proschel M. 2002. The tripotential glial-restricted precursor (GRP) cell and glial development in the spinal cord: Generation of bipotential oligodendrocyte-type-2 astrocyte progenitor cells and dorsal-ventral differences in GRP cell function. J Neurosci 22:248–256.

Gumpel M, Lachapelle F, Gansmuller A, Baulac M, Baron van Evercooren A, Baumann N. 1987. Transplantation of human embryonic oligodendrocytes into shiverer brain. Ann N Y Acad Sci 495:71–85.

Han SS, Liu Y, Tyler-Polsz C, Rao MS, Fischer I. 2004. Transplantation of glial-restricted precursor cells into the adult spinal cord: Survival, glial-specific differentiation, and preferential migration in white matter. Glia 45:1–16.

Iannotti C, Li H, Yan P, Lu X, Wirthlin L, Xu XM. 2003. Glial cell line-derived neurotrophic factor-enriched bridging transplants promote propriospinal axonal regeneration and enhance myelination after spinal cord injury. Exp Neurol 183:379–393.

Jacobs LD, Cookfair DL, Rudick RA, Herndon RM, Richert JR, Salazar AM, Fischer JS, Goodkin DE, Granger CV, Simon JH, Alam JJ, Bartoszak DM, Bourdette DN, Braiman J, Brownscheidle CM, Coats ME, Cohan SL, Dougherty DS, Kinkel RP, Mass MK, Munschauer FE, 3rd, Priore RL, Pullicino PM, Scherokman BJ, Whitham RH. 1996. Intramuscular interferon beta-1a for disease progression in relapsing multiple sclerosis. The Multiple Sclerosis Collaborative Research Group (MSCRG). Ann Neurol 39:285–294.

Janowski M, Walczak P, Date I. 2010. Intravenous route of cell delivery for treatment of neurological disorders. A meta-analysis of preclinical results. Stem Cells Dev 19:5–16.

Kazatchkine MD, Kaveri SV. 2001. Immunomodulation of autoimmune and inflammatory diseases with intravenous immune globulin. N Engl J Med 345:747–755.

Keirstead HS, Nistor G, Bernal G, Totoiu M, Cloutier F, Sharp K, Steward O. 2005. Human embryonic stem cell-derived oligodendrocyte progenitor cell transplants remyelinate and restore locomotion after spinal cord injury. J Neurosci 25(19):4694–705.

Kerr DA, Ayetey H. 2002. Immunopathogenesis of acute transverse myelitis. Curr Opin Neurol 15:339–347.

Kerschensteiner M, Stadelmann C, Buddeberg BS, Merkler D, Bareyre FM, Anthony DC, Linington C, Bruck W, Schwab ME. 2004. Targeting experimental autoimmune encephalomyelitis lesions to a predetermined axonal tract system allows for refined behavioral testing in an animal model of multiple sclerosis. Am J Pathol 164:1455–1469.

Krishnan C, Kaplin AI, Pardo CA, Kerr DA, Keswani SC. 2006. Demyelinating disorders: Update on transverse myelitis. Curr Neurol Neurosci Rep 6:236–243.

Lucchinetti CF, Brueck W, Rodriguez M, Lassmann H. 1998. Multiple sclerosis: Lessons from neuropathology. Semin Neurol 18:337–349.

Maragakis NJ, Rao MS, Llado J, Wong V, Xue H, Pardo A, Herring J, Kerr D, Coccia C, Rothstein JD. 2005. Glial restricted precursors protect against chronic glutamate neurotoxicity of motor neurons in vitro. Glia 50:145–159.

Mothe AJ, Tator CH. 2008. Transplanted neural stem/progenitor cells generate myelinating oligodendrocytes and Schwann cells in spinal cord demyelination and dysmyelination. Exp Neurol 213:176–190.

Murray JA, Blakemore WF. 1980. The relationship between internodal length and fibre diameter in the spinal cord of the cat. J Neurol Sci 45:29–41.

Narayanan SP, Flores AI, Wang F, Macklin WB. 2009. Akt signals through the mammalian target of rapamycin pathway to regulate CNS myelination. J Neurosci 29:6860–6870.

Raine CS. 1997. The Norton Lecture: A review of the oligodendrocyte in the multiple sclerosis lesion. J Neuroimmunol 77:135–152.

Rao MS, Noble M, Mayer-Proschel M. 1998. A tripotential glial precursor cell is present in the developing spinal cord. Proc Natl Acad Sci USA 95:3996–4001.

Saito M, Kitamura H, Sugiyama K. 2001. The specificity of monoclonal antibody A2B5 to c-series gangliosides. J Neurochem 78:64–74.

Sandrock RW, Wheatley W, Levinthal C, Lawson J, Hashimoto B, Rao M, Campanelli JT. 2010. Isolation, characterization and preclinical development of human glial-restricted progenitor cells for treatment of neurological disorders. Regen Med 5:381–394.

Setzu A, Lathia JD, Zhao C, Wells K, Rao MS, Ffrench-Constant C, Franklin RJ. 2006. Inflammation stimulates myelination by transplanted oligodendrocyte precursor cells. Glia 54:297–303.

Talbott JF, Cao Q, Enzmann GU, Benton RL, Achim V, Cheng XX, Mills MD, Rao MS, Whittemore SR. 2006. Schwann cell-like differentiation by adult oligodendrocyte precursor cells following engraftment into the demyelinated spinal cord is BMP-dependent. Glia 54:147–159.

Talbott JF, Loy DN, Liu Y, Qiu MS, Bunge MB, Rao MS, Whittemore SR. 2005. Endogenous Nkx2.2+/Olig2+ oligodendrocyte precursor cells fail to remyelinate the demyelinated adult rat spinal cord in the absence of astrocytes. Exp Neurol 192:11–24.

Tyler WA, Gangoli N, Gokina P, Kim HA, Covey M, Levison SW, Wood TL. 2009. Activation of the mammalian target of rapamycin (mTOR) is essential for oligodendrocyte differentiation. J Neurosci 29:6367–6378.

Walczak P, Kedziorek DA, Gilad AA, Barnett BP, Bulte JW. 2007. Applicability and limitations of MR tracking of neural stem cells with asymmetric cell division and rapid turnover: The case of the shiverer dysmyelinated mouse brain. Magn Reson Med 58:261–269.

Walczak P, Zhang J, Gilad AA, Kedziorek DA, Ruiz-Cabello J, Young RG, Pittenger MF, van Zijl PC, Huang J, Bulte JW. 2008. Dual-modality monitoring of targeted intraarterial delivery of mesenchymal stem cells after transient ischemia. Stroke 39:1569–1574.

Windrem MS, Schanz SJ, Guo M, Tian GF, Washco V, Stanwood N, Rasband M, Roy NS, Nedergaard M, Havton LA, Wang S, Goldman SA. 2008. Neonatal chimerization with human glial progenitor cells can both remyelinate and rescue the otherwise lethally hypomyelinated shiverer mouse. Cell Stem Cell 2:553–565.